Available online at www.sciencedirect.com
ScienceDirect
Catena 73 (2008) 249–260
CATENA
www.elsevier.com/locate/catena

The effectiveness of airborne LiDAR data in the recognition of channel-bed morphology

Marco Cavalli [a,*], Paolo Tarolli [b], Lorenzo Marchi [a], Giancarlo Dalla Fontana [b]

[a] CNR-IRPI, Corso Stati Uniti 4, 35127 Padova, Italy
[b] Department of Land and Agroforest Environments University of Padova, Agripolis, viale dell'Università 16, 35020 Legnaro (PD), Italy

Received 11 June 2007; received in revised form 2 November 2007; accepted 5 November 2007

Abstract

High-resolution topographic data have the potential to differentiate the main morphological features of a landscape. This paper analyses the capability of airborne LiDAR-derived data in the recognition of channel-bed morphology. For the purpose of this study, 0.5 m and 1 m resolution Digital Terrain Models (DTMs) were derived from the last pulse LiDAR data obtained by filtering the vegetation points. The analysis was carried out both at 1-D scale, i.e. along the longitudinal channel profile, and at 2-D scale, taking into account the whole extent of the channel bed. The 1-D approach analyzed the residuals of elevations orthogonal to the regression line drawn along the channel profile and the standard deviation of local slope. The 2-D analysis was based on two roughness indexes, consisting on the local variability of the elevation and slope of the channel bed. The study was conducted in a headwater catchment located in the Eastern Italian Alps. The results suggested a good capability of LiDAR data in the recognition of river morphology giving the potential to distinguish the riffle-pool and step-pool reaches.

Keywords: DTM; LiDAR; Surface roughness; Channel-bed morphology; Step pools

1. Introduction

The airborne laser altimetry technology (LiDAR, Light Detection And Ranging) provides high-resolution topographical data, which can significantly contribute to a better representation of land surface. A valuable characteristic of this technology, which marks advantages over the traditional topographic survey techniques, is the capability to derive a high-resolution Digital Terrain Model (DTM) from the last pulse LiDAR data by filtering the vegetation points (Slatton et al., 2007).

In the field geo-hydrological hazards in mountainous areas, it is possible to mention the use of LiDAR data for the characterisation of large landslides, as the basis for numerical modelling of shallow landslides, for the recognition of depositional features on alluvial fans and for the study of the longitudinal profile of rivers. Anyway, the use of LiDAR technology for these types of quantitative analyses is relatively new.

In previous studies, LiDAR elevation data were used to evaluate the surface roughness as a useful approach to detect landslide areas (McKean and Roering, 2004), and to characterize and differentiate the landslide morphology and activity (Glenn et al., 2006). Tarolli and Tarboton (2006) used LiDAR-derived DTMs to identify the optimal size of the cell for the assessment of shallow landslides.

Staley et al. (2006) used LiDAR-derived topographic attributes (profile curvature and surface gradient) at high resolution, for differentiating deposition zones on debris flow fans. Frankel and Dolan (2007) combined quantitative measures of surface roughness, obtained from LiDAR data, with classic methods of geomorphology and sedimentology to characterise and differentiate alluvial fan surfaces with different relative ages. Storesund and Minear (2006) analyzed the river geomorphology and river restoration by LiDAR data. Magirl et al. (2005) evaluated the long-term changes created by fluvial and debris flow activity in the Colorado River along the Grand Canyon (USA). The topographic data available for the study of Magirl et al. (2005) were a LiDAR flight of 2000 and a

* Corresponding author. Tel.: +39 0498295820; fax: +39 0498295827.
E-mail address: marco.cavalli@irpi.cnr.it (M. Cavalli).

0341-8162/$ - see front matter © 2007 Elsevier B.V. All rights reserved.
doi:10.1016/j.catena.2007.11.001

historical topographic survey made in 1923 using theodolite and stadia techniques. Topographic data were correlated to the LiDAR data at given points along the river, thus making possible the assessment of the changes that had occurred in other parts of the surveyed area. With regard to the application of LiDAR techniques in the recognition of small, ephemeral channels, the study of James et al. (2006) has proven the capability of LiDAR data in identifying and mapping gullies and headwater streams, even under forest cover. Terrestrial LiDAR can be applied at the local scale of individual test areas in channel beds: Smart et al. (2004) have demonstrated the suitability of a portable hand-held laser scanner for obtaining accurate Digital Terrain Models of alluvial channels.

The studies cited above used LiDAR data to analyze various topics regarding the topography of slopes and channel networks. This paper focuses on a specific objective: to analyze the capability of high-resolution LiDAR data in the recognition of morphological features of channel bed in a headwater alpine catchment. The paper is divided into five sections. Section 2 describes the study area, a small catchment located in the Eastern Italian Alps where LiDAR elevation data were available. In Section 2 also the LiDAR data specifications are reported. Section 3 describes the methodologies adopted in the analysis. Sections 4 and 5, respectively, present and discuss the results. Section 6, finally, shows a summary of our findings.

2. Study area

The study area is the Cordon catchment (Figs. 1 and 2), located in the Dolomites, a mountain region of Eastern Italian Alps. The extraction of the basin from the DTM and the assessment of its principal morphometric parameters have been made by the open source TauDEM software package (http://www.engineering.usu.edu/dtarb/taudem) at 1 m grid size LiDAR-derived DTM. The basin covers 5 km^2, the elevation ranges between 1763 and 2748 m a.s.l., with an average value of 2200 m a.s.l. The basin is highly dissected with hillslope lengths on the order of 40–60 m. Average slope is 27°, slopes of 30–40° are common, and there is a substantial number of slopes that locally exceed 45°, including subvertical cliffs in the upper part of the basin. The geological settings of the basin are rather complex: dolomites rocks crop out in the upper part, whereas in the central and lower parts volcanic conglomerates, sandstones and calcareous-marly rocks crop out; moraines, scree deposits and landslide accumulations are also widespread. The basin morphologically is divided into three parts (Friz et al., 1992): 1) the upper part consists of dolomite outcrops and talus slopes bordering the cliffs (A in Fig. 1); 2) the middle part consists of a low-slope belt, whose lower edge corresponds to a sudden increase of slope; this morphological threshold is crossed by the Rio Cordon in a steep rocky gorge (B in Fig. 1); 3) the lower part of the Rio Cordon basin displays steep slopes and a narrow valley (C in Fig. 1). The area presents a mean annual rainfall of about 1100 mm; precipitation occurs mainly as snowfall from November to April. Runoff is dominated by snowmelt in May and June; summer and early autumn floods represent an important contribution to the flow regime. In summer, storm events are sometimes separated by long dry spell. Vegetation cover consists mainly of mountain grassland (61%); shrubs are rather widespread (18%), while forest stands composed by

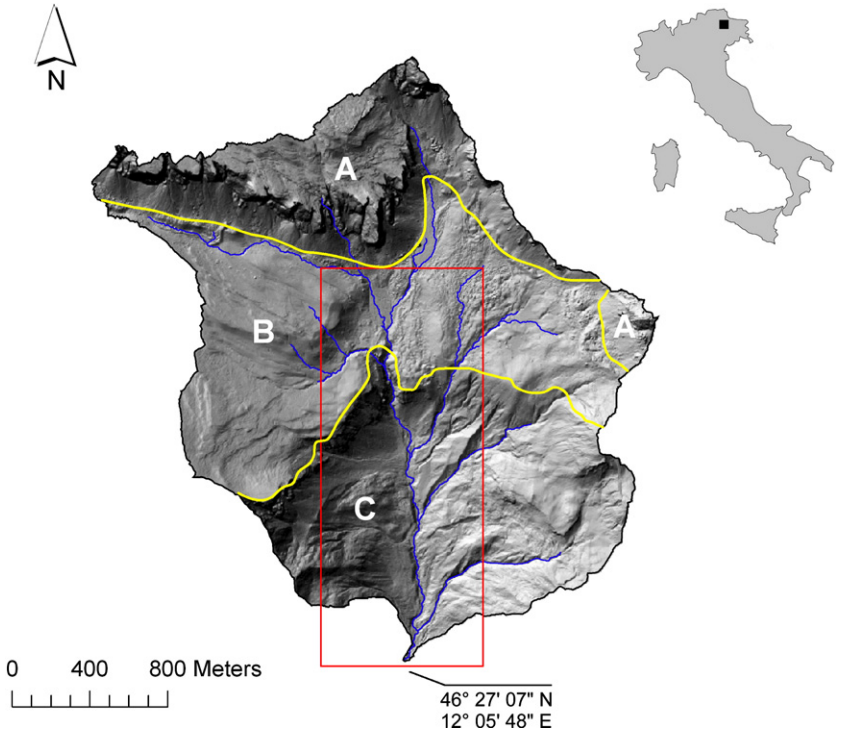

Fig. 1. Location map of the study area. Letters indicate the three morphologically divided areas of the Rio Cordon basin (A: rocky outcrops and talus slopes; B: low-slope belt; C: steep slopes and narrow valley area). The rectangle highlights the extent of Fig. 3.

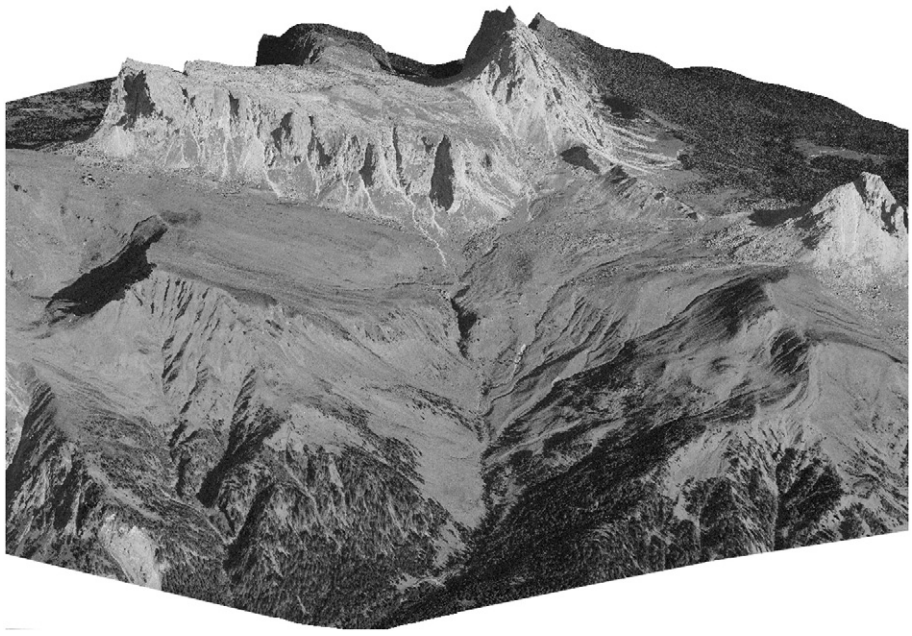

Fig. 2. Image of the Rio Cordon basin provided by draping a digital orthophoto of 2003 over a 40 m Digital Elevation Model.

Norway spruce and European larch are found only in the lower part of the watershed and occupy 7% of the total area. Differently from many alpine torrents, in which control works (check dams, channel lining, etc.) have extensively been built, no artificial structures are present in the headwaters of the Rio Cordon, where channel morphology reflects natural interactions between hydrology, geological settings, and sediment supply. The Rio Cordon basin was also chosen as a study area because the morphology of the main stream has been deeply investigated in previous studies (Billi et al., 1998; Lenzi et al., 1999; Lenzi, 2001), in addition to LiDAR data availability.

2.1. The analyzed channel

In our study, we refer to the morphological and topographic analysis of channel bed of the Rio Cordon reported by Lenzi (2001). The paper by Lenzi (2001) presents a classification of the channel-bed morphology (Fig. 3) and reports the geometric parameters of step-pool structures, measured using a total station.

In this study, the main channel reach, starting from the low-slope belt in the central part of the basin, where some headwater streams merge into the main channel (B in Fig. 1), and ending to the basin outlet was considered (Fig. 1). The analyzed channel reach has a total length of about 2725 m and ranges in elevation from 1765 to 2162 m (Fig. 3). The main channel of Rio Cordon is quite stable and can be modified only by large floods, which have not occurred in the period between bed-morphology surveys (Lenzi, 2001) and the LiDAR survey. The bankfull width, determined by aerial photo-interpretation and shaded relief map, presents a mean value of about 7 m ranging from a minimum 2.5 m to 22 m. The Rio Cordon shows a complex alternation of different morphologies (Figs. 3 and 4). Looking at the Fig. 3, from the upper end of the main channel, we find a riffle-pool reach, a bedrock stretch corresponding to the gorge between the middle and the lower part of the basin, a cascade reach at the outlet of the rocky gorge, two riffle-pool sequences, separated by a short mixed reach, and an alternation of eight step-pool and eight mixed reaches in the lower part of the stream. Step-pool and mixed morphology have an average length of 45 and 42 m, respectively.

The riffle-pool reaches are rarely found when the channel gradient exceeds 3–5% (Rosgen, 1994; Montgomery and Buffington, 1997). Step-pool sequences are mostly found within a gradient range between 2 and 20% (Chin and Wohl, 2005; Wilcox and Wohl, 2007). Steps are typically formed from accumulations of boulders and cobbles, which span the channel in a more or less continuous line and separate a backwater pool upstream from a plunge pool downstream. The mixed reaches are step-pool sequences irregularly punctuated by small heaps of coarse material (Lenzi et al., 1999). Mixed reaches are similar to step-pool reaches but with coarse particles bars deposited upstream of the boulder steps, or adjacent isolated big boulders, and largely infilling the upstream end of pools (Billi et al., 1998).

The classification of the Rio Cordon into step-pool, mixed and riffle-pool reaches (Fig. 3) has been used for assessing the capability of LiDAR in recognising morphological settings of the channel bed.

2.2. LiDAR data specifications

The LiDAR and photographic data (provided by Helica srl) were acquired from a helicopter using an ALTM 3100 OPTECH, and Rollei H20 Digital camera flying at an average altitude of 1000 m above ground level during snow free

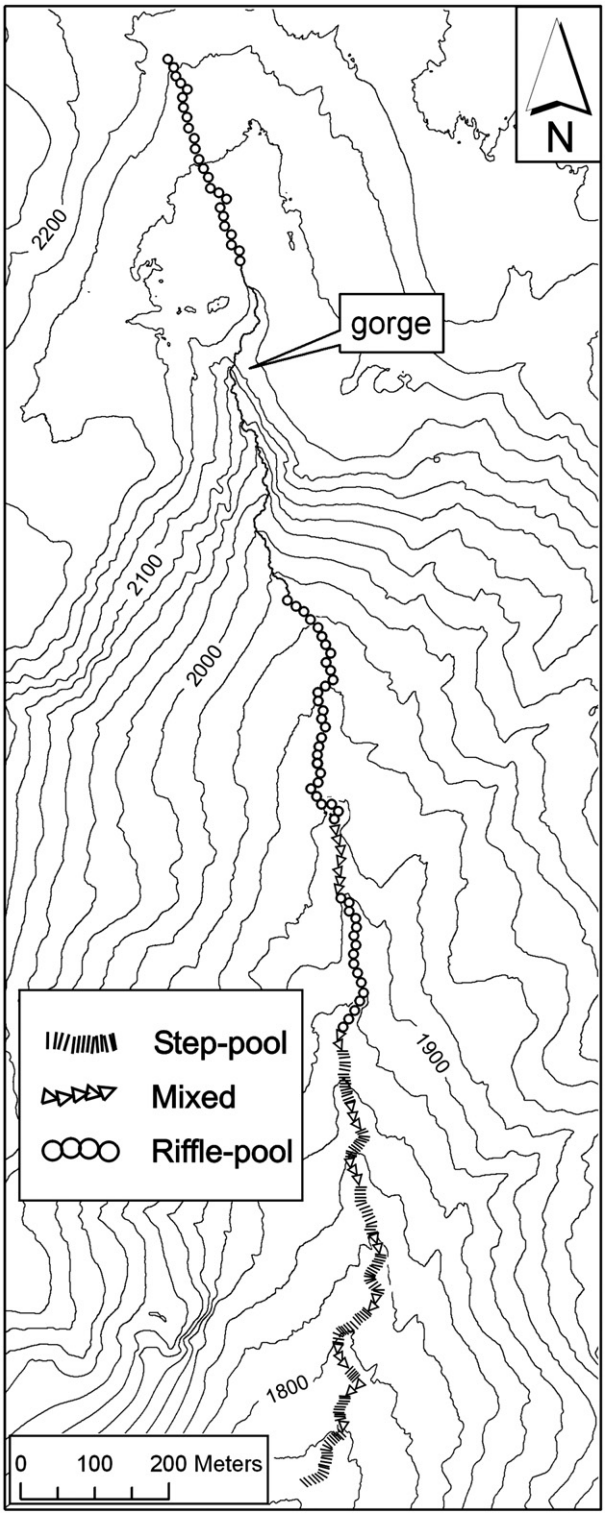

Fig. 3. Plan view of the main stream showing the classification of channel morphology.

conditions in October 2006. The flying speed was 80 knots, the scan angle 20° and the pulse rate 71 kHz. The survey design point density was specified to be greater than 5 points/m^2, recording up to 4 returns, including first and last. LiDAR point measurements were filtered into returns from vegetation and bare ground using the Terrascan™ software classification routines and algorithms. The shallow depth of water in the analyzed stream at the time of LiDAR flight (not exceeding few tens of centimetres) had made it possible the survey of the channel bed without using a bathymetric LiDAR sensor.

3. Methods

The LiDAR bare ground points were used for the DTM interpolation at 0.5 m and 1 m grid resolution, which was carried out using the ArcGIS TOPOGRID tool. The TOPOGRID algorithm (Hutchinson, 1989) is a spline technique that uses slope rather than curve information as penalty function. The DTM with resolution of 0.5 m has the capability to give a better representation of the topographic surface, showing also the less evident morphological features. The 1 m grid size was taken into consideration in order to test the influence of DTM cell size on the analysis of channel morphology. DTMs with larger cells were not considered because the cell size would be too close to the minimum width of the channel, thus preventing the application of the methods devised for this study. The channel reach has been analysed at both 1-D and 2-D scales: the 1-D analysis deals with the recognition of topographic features along the talweg, the 2-D analysis considers also the cross-sectional extent of the channel bed.

3.1. 1-D analysis

In order to extract objectively the longitudinal channel profile from the DTM, the following procedure was used: i) the local depressions (pits) were removed using TauDEM tool which identifies all pits in the DTM and raises their elevation to the level of the lowest pour point around their edge; ii) the flow directions were determined by the D8 algorithm (O'Callaghan and Mark, 1984), and the channel network was extracted adopting a constant threshold area; iii) the cells corresponding to the main channel were used to extract the longitudinal profile from the original (i.e. non depitted) DTM. The original DTM has the potential to show correctly local depressions in the channel surface, such as the pools amongst steps. The depitted DTM was used only as the basis for the extraction of the stream profile. This procedure was preferred to the visual tracing of the talweg line because it avoids possible subjectivities in the interpretation of aerial photographs.

An index aimed at expressing the local variability of elevations along the talweg was derived. The analysis was based on the computation of the residuals between the elevations points of longitudinal profile and the related linear regression line. The linear regression was performed on reaches of constant slope, with length not exceeding 100 m. Such short channel reaches display straight longitudinal profiles, which can effectively be interpolated by a linear regression, so that the residuals from the regression line can be referred to the local roughness, excluding the influence of topographic variations at a larger scale. In order to remove the effect of the channel slope expressed by the angular coefficient of the regression equation, the residuals were computed orthogonally to the regression line

Fig. 4. The three morphological units. SP: step pool; M: mixed; RP: riffle pool.

($y\,y''$ in Fig. 5). The local variability of the elevations was given by the standard deviation of residuals calculated on intervals of 2.5 m and 5 m for the 0.5 m and 1 m profiles, respectively.

A second indicator of topographic variability, given by the standard deviation of local slopes, computed on the same intervals of the previous analysis, was also tested.

The Mann–Whitney *U* test (Statsoft, 2001) was then applied to check if the different morphological units observed in the Rio Cordon (step-pool, riffle-pool, and mixed reaches) display significant differences in the local variability of elevation and slope, expresses by the standard deviation of the residuals from the regression lines and the standard deviation of local slope.

3.2. 2-D analysis

The 2-D analysis was based on the calculation of two roughness indexes, used to measure the variability of elevation and slope in local patches of the DTM. The potential behind the 2-D analysis is to relate values of the roughness indexes to channel reach morphology. The comparison of these indexes related to each channel morphology unit was carried out by the Mann–Whitney *U* test.

3.2.1. Roughness index-elevation

Several methods have been proposed to measure the surface roughness by LiDAR data (e.g. McKean and Roering, 2004; Haneberg et al., 2005; Glenn et al., 2006; Frankel and Dolan, 2007). In this work we define "roughness index-elevation" as the standard deviation of residual topography. A neighbourhood analysis was used to derive the roughness index of the analyzed channel bed. This method computes an output grid where the value at each location is a function of the input cells within a specified neighbourhood. Fig. 6 shows the flow chart of the calculation of the roughness index-elevation. A smoothed

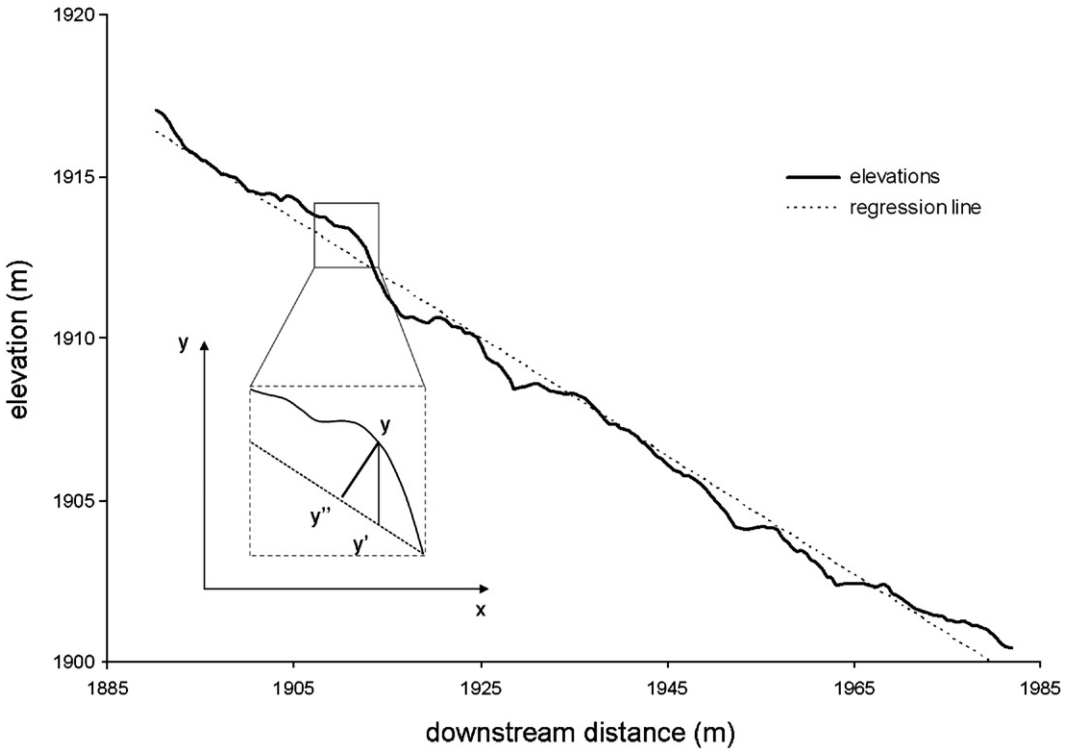

Fig. 5. Assessment of the residuals orthogonal to the regression line (example for a step-pool reach).

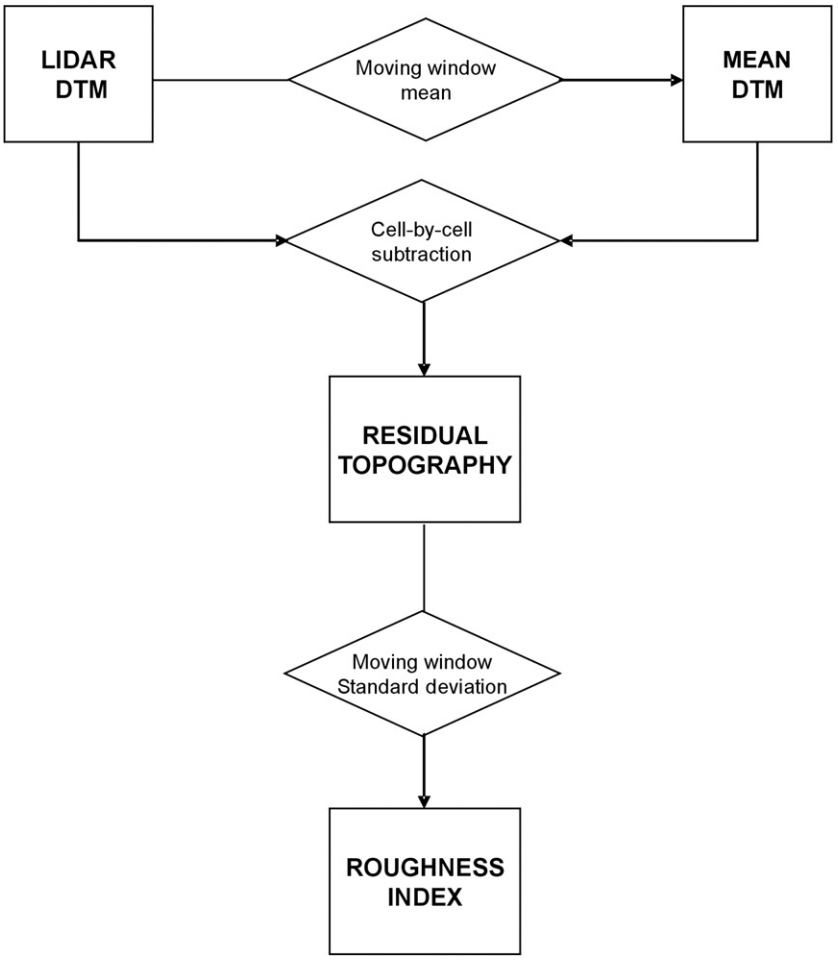

Fig. 6. Flow chart of the calculation of the roughness index-elevation.

version of the LiDAR DTM (mean DTM in Figs. 6 and 7) was created by averaging value within a 5-cells moving window. Each cell of the mean DTM has a value corresponding to the mean of the 25 neighbourhood cells values of the LiDAR DTM. The grid of residual topography was then calculated as the cell-by-cell difference between the LiDAR DTM and the mean DTM. Finally, the standard deviations of residual topography values are computed in a 5-cells moving window over the

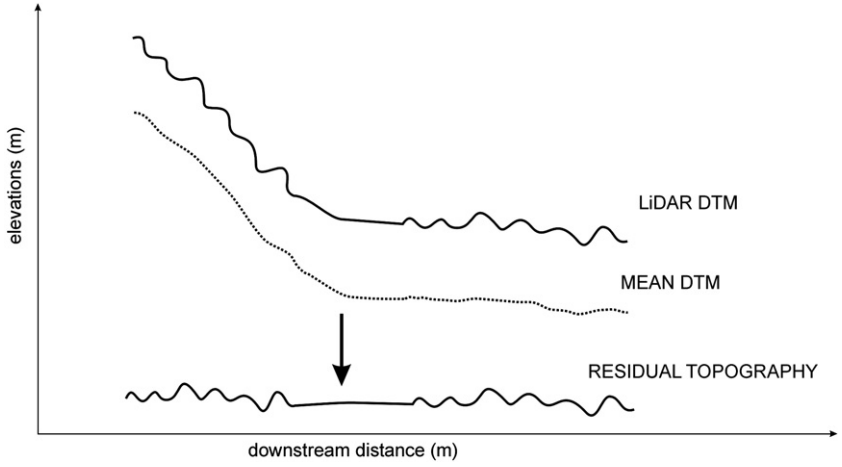

Fig. 7. One-dimensional example of the residual topography calculation. The dotted line is the profile of the mean DTM calculated over the LiDAR DTM (continuous line) with neighbourhood analysis approach. Residual topography is calculated as the difference between LiDAR DTM and mean DTM.

residual topography grid. The roughness index-elevation is computed as:

$$\sigma = \sqrt{\frac{\sum_{i=1}^{25}(x_i - x_m)^2}{25}} \quad (1)$$

where σ is the roughness index-elevation or the standard deviation of residual topography, 25 is the number of the processing cells within the 5-cells moving window, x_i is the value of one specific cell within the moving window, x_m is the mean of the 25 cells values.

The resulting roughness value for each grid cell expresses the topographic variability over length scales from 0.5 m (grid size) to 2.5 m (moving window size) when it is calculated on the 0.5 m grid size DTM, and 1 m to 5 m when it is calculated on the 1 m grid size DTM. Fig. 7 shows the calculation of the residual topography grid in a idealized one-dimensional profile. The calculation of the surface roughness by means of the residual topography grid provides a measure of this index independent from the effect of slope along the channel.

3.2.2. Roughness index-slope

Similarly to the 1-D analysis, we calculated also an indicator based on the variability of slope (roughness index-slope). This second indicator of topographic variability is given by the standard deviation of slope. A map of local slopes, calculated in the direction of the steepest descent according to the D8 flow direction was derived from the DTM. The standard deviation of slope was then computed within a 5-cells moving window.

3.3. Space scales of the analysis

The space intervals for the calculation of the surface roughness were chosen taking into account the size of the topographic features under study. In particular, the choice was done focusing on the step-pool morphology, which is the most heterogeneous of the three channel types investigated. As stated before, both 1-D and 2-D analyses express the topographic variability over length scales from the grid size (0.5 m and 1 m) to the interval in which the roughness is calculated. An equal interval was adopted for both 1-D and 2-D analyses (5 times the grid size of the DTM). In the case of the 2-D analysis, the interval of calculation of the roughness index is given by the moving window size. In this study, the topographic variability in an interval of 0.5–2.5 m (in the case of 0.5 m grid size DTM) and 1–5 m (in the case of 1 m grid size DTM) is thus investigated. According to the study of Lenzi (2001), the grain size of risers in the step pools of the Rio Cordon has D_{50} of about 0.6–0.8 m and D_{84} of about 1.0 m. These values have been considered to identify the DTMs grid size that corresponds to the lower limits of the analysis (0.5 m and 1 m). The upper limits are thus based on the values of mean step-pool spacing reported by Lenzi (2001) that range from about 2.5 to 5 m (only in few cases mean step-pool spacing was observed larger than 5 m). Performing the

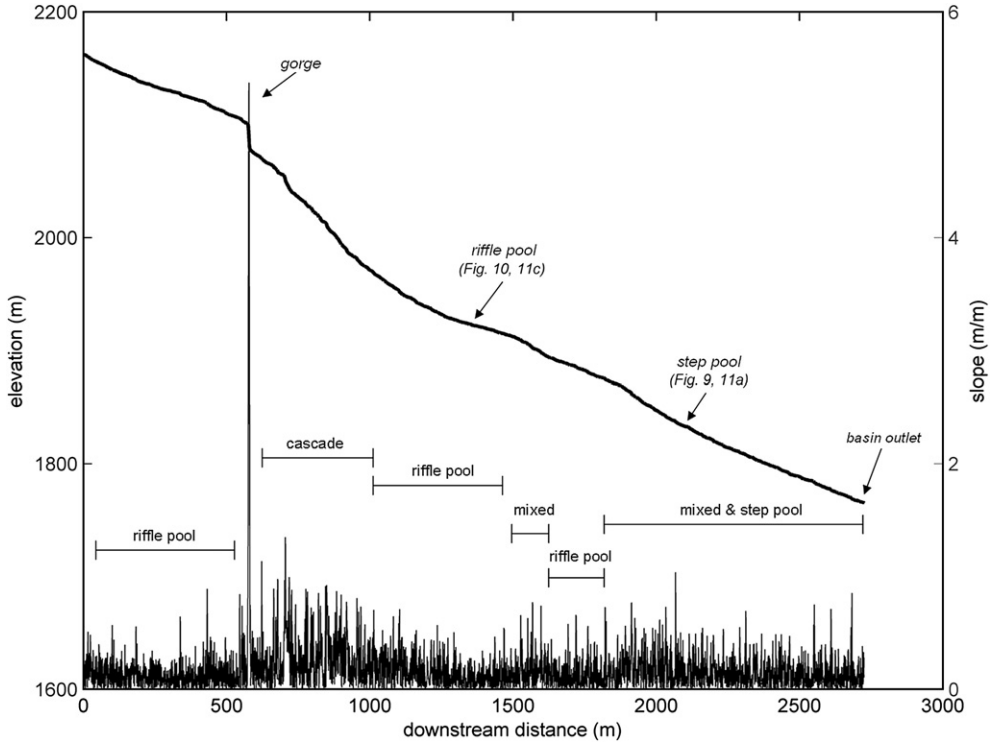

Fig. 8. Longitudinal profile of the studied channel and pattern of the local slope (absolute value).The plot shows the different morphological units along the channel and the location of the step-pool and riffle-pool reach described in the Figs. 9, 10, and 11.

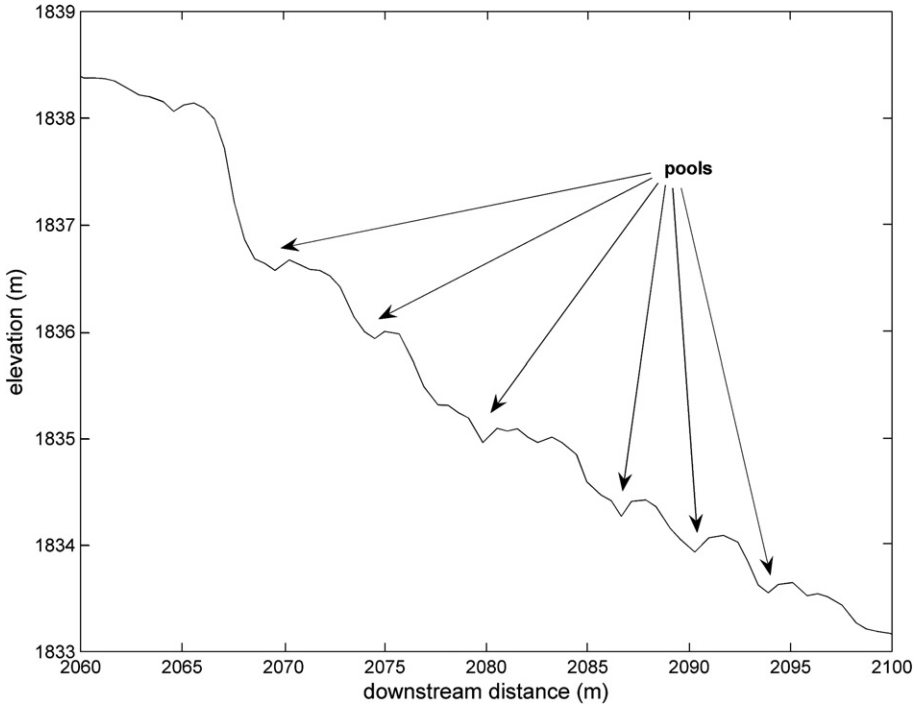

Fig. 9. Channel profile for a step-pool reach (0.5 m DTM).

analyses with a moving window size larger than 5 m would lead to smoothing out step-pool reaches.

4. Results

Fig. 8 shows the longitudinal profile of the analyzed channel and the pattern of local slope. In order to better show the pattern of slope along the channel, absolute values are presented in Fig. 8 (the local slope can be negative in the step-pool reaches). Abrupt changes in local slope correspond to variations in the morphological features of channel reaches. Generally, low-slope reaches are related to riffle-pool morphology units and high-slope reaches (especially those sited in proximity of basin outlet) to steep-pool or mixed units. The highest values of slope

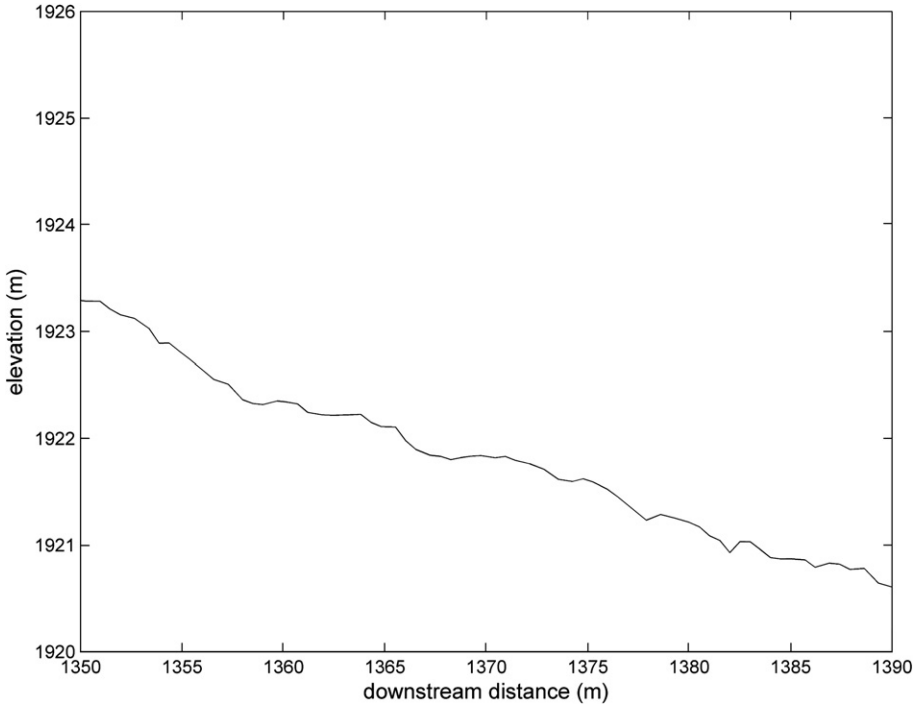

Fig. 10. Channel profile for a riffle-pool reach (0.5 m DTM).

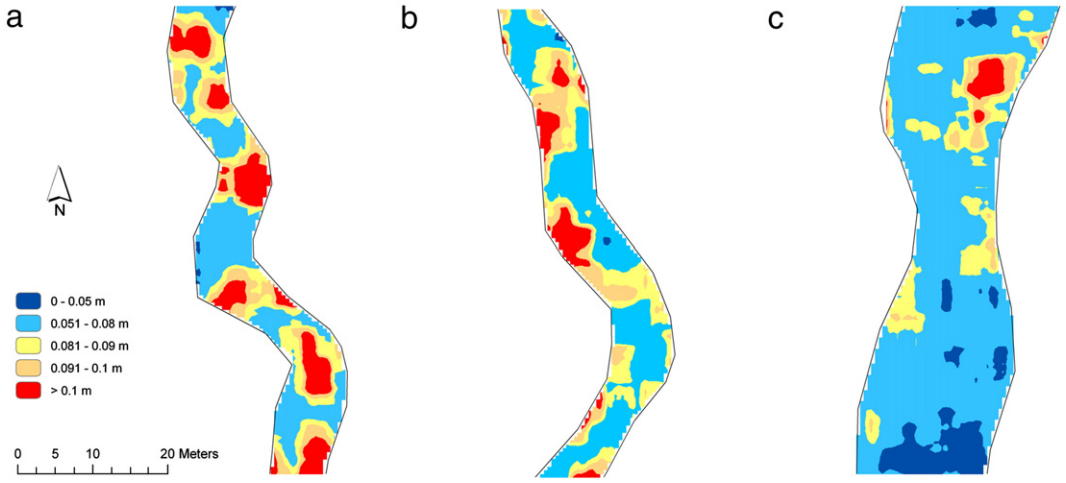

Fig. 11. Roughness index-elevation for a step-pool channel reach (a), a mixed reach (b) and a riffle-pool reach (c) (0.5 m DTM).

correspond to the rocky gorge and to a cascade reach located immediately downstream. Figs. 9 and 10 show the longitudinal channel profile respectively for a step-pool and riffle-pool reach. The pools in Fig. 9 are clearly detected among the steps. The difference with riffle-pool morphology (Fig. 10), less steep and relatively smooth, is evident. Fig. 11 shows the roughness

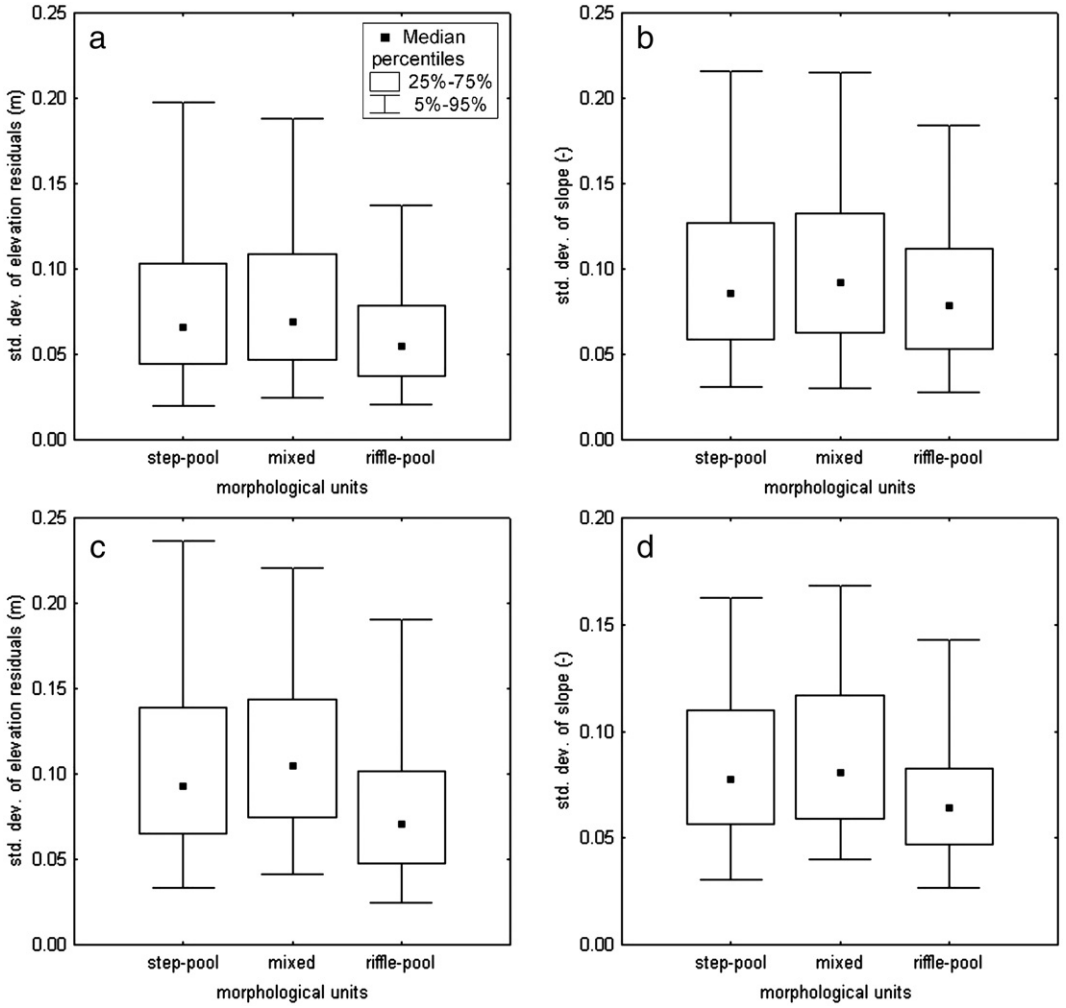

Fig. 12. Comparison of channel morphologies for 1-D analysis: standard deviation of residuals from the linear regression line of the channel profile (DTM size of 0.5 m) (a), standard deviation of slope along the channel profile (DTM size of 0.5 m) (b), standard deviation of residuals from the linear regression line of the channel profile (DTM size of 1 m) (c) and standard deviation of slope along the channel profile (DTM size of 1 m) (d).

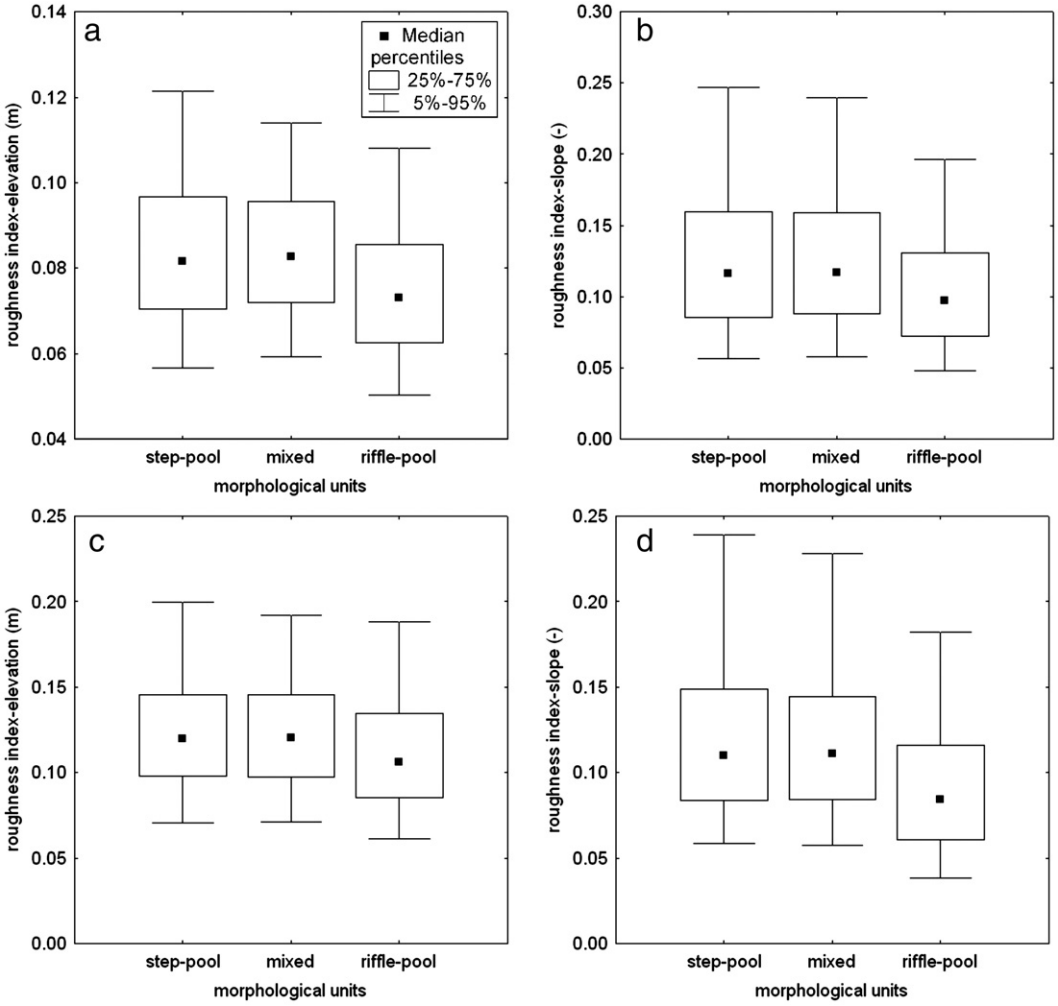

Fig. 13. Comparison of channel morphologies for 2-D analysis: roughness index-elevation of channel surface (DTM size of 0.5 m) (a), roughness index-slope of the channel surface (DTM size of 0.5 m) (b), roughness index-elevation of channel surface (DTM size of 1 m) (c), and roughness index-slope of the channel surface (DTM size of 0.5 m) (d).

index-elevation respectively for a step-pool (Fig. 11a), mixed (Fig. 11b) and riffle-pool (Fig. 11c) reach. The index displays higher values and a greater variability in the step-pool reach.

Fig. 12 presents box plots of the 1-D analysis carried out using the standard deviation of the residuals from the regression line drawn along the channel profile (Fig. 12a and c) and the standard deviation of slope values along the talweg (Fig. 12b and d), for 0.5 m and 1 m cell size, respectively.

Fig. 13 presents box plots of the 2-D analysis showing the results of the roughness index-elevation (Fig. 13a and c) and the roughness index-slope (Fig. 13b and d). In the Fig. 12, the step-pool and mixed reaches present higher values of the median than the riffle-pools both for standard deviation of the residuals and standard deviation of slope along the talweg. The greatest value for the step-pool and mixed reaches is due to the abrupt changes in elevations of these morphologies. On the contrary,

Table 1
Comparison of morphological units (1-D analysis): results of the Mann–Whitney *U* test (significance level $\alpha = 0.05$)

Channel morphology	0.5 m DTM		1 m DTM	
	Residual analysis *p*-value	Slope analysis *p*-value	Residual analysis *p*-value	Slope analysis *p*-value
SP–RP	<0.001	<0.001	<0.001	<0.001
SP–M	0.132	0.118	0.027	0.186
M–RP	<0.001	<0.001	<0.001	<0.001

SP: step-pool; M: mixed; RP: riffle-pool.

Table 2
Comparison of morphological units (2-D analysis): results of the Mann–Whitney *U* test (significance level $\alpha = 0.05$)

Channel morphology	0.5 m DTM		1 m DTM	
	Roughness index-elevation *p*-value	Roughness index-slope *p*-value	Roughness index-elevation *p*-value	Roughness index-slope *p*-value
SP–RP	<0.001	<0.001	<0.001	<0.001
SP–M	0.021	0.090	0.898	0.902
M–RP	<0.001	<0.001	<0.001	<0.001

SP: step-pool; M: mixed; RP: riffle-pool.

the smoother profile of the riffle-pool reaches is reflected in lower values. Similar results can be observed in the case of the 2-D analysis (Fig. 13). The mixed reaches values of the roughness indexes are similar to the step-pools reaches. The riffle-pool reaches present lower values of the 2-D indexes due to the smoother surface profile.

The results of the statistical analysis are reported in Tables 1 and 2. Comparison of morphological units for both 0.5 m and 1 m DTMs shows a highly statistically significant difference ($\alpha = 0.05$) between step-pool and riffle-pool and mixed and riffle-pool reaches. No significant differences between step-pool and mixed morphological units arise from all the analysis except in the case of the elevation residuals analysis of 1 m DTM and the roughness index-elevation analysis of 0.5 m DTM.

5. Discussion

The results of statistical analyses indicate that step-pool and riffle-pool reaches have distinctive surface roughness values (Tables 1 and 2). Step-pools typically exhibit higher values for all the adopted methods than riffle-pools. The smoother profile of riffle-pool reaches is differentiated from mixed reaches, as well (Figs. 12 and 13). The lack of statistically significant differences between mixed and step-pool reaches is not surprising, because mixed reaches can be viewed as a variant of step-pools, and the recognition of these two morphologies in the field requires the skills of an experienced observer (Fig. 4). Moreover, the comparison of the medians of the roughness indexes, carried out through the Mann–Whitney *U* test, does not consider the spatial distribution of the roughness within the investigated areas. In Fig. 11 it can be observed that the highest roughness values, related to the risers of boulders, are transversally arranged in the step-pool reach, whereas they are irregularly scattered in the mixed reach, where they correspond to isolated big boulders and coarse particle bars.

The classification of morphological channel units has been carried out in the Rio Cordon using indicators of the local variability of the elevation: the residuals from a linear interpolation of the channel profile and the roughness index-elevation. The use of these indicators makes it possible to separate the influence of local variability of surface, which characterizes channel-bed morphologies, from that of channel slope at a larger space scale, which mostly depends on general morphological and structural settings of the basin.

The indicators of topographic roughness based on slope variability give results consistent with those related to elevation variability. In the case of 1-D analysis, the standard deviation of local slope could be preferred to the analysis of residuals from the linear regression of the longitudinal profile because of easier computation.

Both the 1-D and the 2-D analyses have proved suitable for the comparison between different channel morphologies. The 2-D analysis, differently from the 1-D analysis, does not require the extraction of a longitudinal profile from the DTM. The 2-D assessment of the surface roughness overcomes possible drawbacks associated to the removal of local depressions and to the identification of the flow directions on a depitted DTM. The longitudinal profile of the channel is anyway a classic representation of stream morphology. LiDAR surveys, when they lead to high density data sets, make it possible to draw channel profiles with a detail, which would be unlikely to attain using traditional topographic maps.

No major differences arise between the analysis carried out on the 0.5 m and 1 m DTM. A possible explanation for this fact could be found in the relationship between cell size and particle size of the channel bed. It can be reminded that the grid size of the 1 m DTM is close to the diameter of the largest boulders forming the steps in the Rio Cordon (Lenzi, 2001). This suggests that a 1 m grid cell resolution is able to detect this type of morphology without a major loss of accuracy with respect to finer resolutions. Both grid sizes of DTM used in this study (e.g. 0.5 m and 1 m) have thus the potential to discriminate small features leading to a good estimation of channel morphology.

Flores et al. (2006) stress that DTM resolution often represents a relevant source of error for the estimation of local channel slope. Actually, the cell size of DTMs derived from standard topographic maps is often larger than the width of small mountainous channels. As a consequence, the topography of adjacent side slopes influences the gradient of DTM cells pertaining to the channel network. Some improvement can be obtained when the topographic maps permit obtaining DTMs with cell size close to the channel width (Dalla Fontana and Marchi, 2003). However, even in this case, DTM cells may not correspond exactly to the channel network, so that assessment of slope is prone to the influence of topographic features external to the channel. Moreover, it is difficult to obtain DTMs with cells smaller than 5 m from standard topographic maps, whereas other traditional techniques, such as the photogrammetric restitution of large scale photos, can successfully be applied only in vegetation-free areas. Thanks to the small DTM cell size affordable when high density of ground points is available, a significant contribution can be expected from LiDAR data also in the assessment of local channel slope. It should be stressed, however, that aerial LiDAR is not synonymous of high density of ground data. Inadequate density of data can occur due to poor design of the survey or to the presence of dense vegetation cover, which results in a low density of ground pulse returns.

6. Conclusions

This paper discusses the effectiveness of LiDAR data in the recognition of the Rio Cordon channel-bed morphology. LiDAR-derived DTMs have shown a satisfactory capability in the analysis of the topographic variations within the stream profile. The use of indicators of the local variability of the elevation and slope has allowed to distinguish different channel-bed morphologies such step-pool and riffle-pool reaches. The analysis carried out in the Rio Cordon has also demonstrated that, in boulder-bed mountain torrents, a fine cell resolution of LiDAR-derived DTMs can be close to, or even smaller than, the diameter of the largest particles in the channel bed. This makes it possible the recognition of rather complex morphologies, such as step-pool sequences (Fig. 9).

We remind that the aim of this study was to evaluate the performance of LiDAR data in the recognition channel-bed morphology. This has been carried out by comparing morphometric indexes derived from LiDAR-based DTMs with a previous classification of channel morphological units, which had been carried out through field surveys. A heuristic use of indexes of surface roughness for the classification of morphological units, without relying on a previous categorization, could represent a further step in the use of LiDAR data for the analysis of channel-bed morphology. The topography of channel beds is normally investigated by means of field surveys. Topographic surveys, carried out using total stations or differential GPS, have an unsurpassed accuracy, which is especially needed for research purposes. Data from airborne LiDAR have proved adequate for a quantitative representation of mountain channel-bed topography. Depending on the accuracy required and on local conditions (e.g. the presence of vegetation on the channel banks), LiDAR data can be considered as a substitute of traditional field survey techniques or as a tool for a preliminary recognition of channel morphology.

Acknowledgements

This study was partly funded by the Italian Ministry of University and Research — GRANT PRIN 2005 "National network of experimental basins for monitoring and modelling of hydrogeological hazard". The authors wish to thank Prof. V. D'Agostino for the careful reading of the manuscript. Finally, the authors wish to acknowledge two anonymous reviewers, and the Joint Editor, Prof. O. Slaymaker, for their valuable comments on the manuscript.

References

Billi, P., D'Agostino, V., Lenzi, M.A., Marchi, L., 1998. Bedload, slope and channel processes in a high-altitude alpine torrent. In: Klingeman, P., Beschta, R.L., Komar, P.D., Bradley, J.B. (Eds.), Gravel-bed Rivers in the Environment. Water Resources Publications, Colorado, pp. 15–38.

Chin, A., Wohl, E., 2005. Toward a theory for step pools in stream channels. Progress in Physical Geography 29 (3), 275–296.

Dalla Fontana, G., Marchi, L., 2003. Slope–area relationships and sediment dynamics in two alpine streams. Hydrological Processes 17 (1), 73–87.

Flores, A.N., Bledsoe, B.P., Cuhaciyan, C.O., Wohl, E.E., 2006. Channel-reach morphology dependence on energy, scale, and hydroclimatic processes with implications for prediction using spatial data. Water Resources Research 42, W06412. doi:10.1029/2005WRR004226.

Frankel, K.L., Dolan, J.F., 2007. Characterizing arid-region alluvial fan surface roughness with airborne laser swath mapping digital topographic data. Journal of Geophysical Research – Earth Surface 112, F02025. doi:10.1029/2006JF000644.

Friz, C., Gatto, G., Silvano, S., 1992. Caratteristiche geolitologiche, geomorfologiche e dissesti. Il bacino attrezzato del Rio Cordon. Quaderni di Ricerca, 13. Centro Sperimentale Valanghe e Difesa Idrogeologica, Regione del Veneto, pp. 15–25 (in Italian).

Glenn, N.F., Streutker, D.R., Chadwick, D.J., Thackray, G.D., Dorsch, S.J., 2006. Analysis of LiDAR-derived topographic information for characterizing and differentiating landslide morphology and activity. Geomorphology 73, 131–148.

Haneberg, W.C., Creighton, A.L., Medley, E.W., Jonas, D., 2005. Use of LiDAR to assess slope hazards at the Lihir gold mine, Papua New Guinea. Proceedings, International Conference on Landslide Risk Management, Vancouver, British Columbia, May–June, 2005. A.A. Balkema, Leiden. Supplementary CD.

Hutchinson, M.F., 1989. A new procedure for gridding elevation and stream line data with automatic removal of spurious pits. Journal of Hydrology 106, 211–232.

James, L.A., Watson, D.G., Hansen, W.F., 2006. Using LiDAR data to map gullies and headwater streams under forest canopy: South Carolina, USA. Catena. doi:10.1016/j.catena.2006.10.010.

Lenzi, M.A., 2001. Step-pool evolution in the Rio Cordon, Northeastern Italy. Earth Surface Processes and Landforms 26 (9), 991–1008.

Lenzi, M.A., D'Agostino, V., Billi, P., 1999. Bedload transport in the instrumented catchment of the Rio Cordon: Part I. Analysis of bedload records, conditions and threshold of bedload entrainment. Catena 36 (3), 171–190.

Magirl, C.S., Webb, R.H., Griffiths, P.G., 2005. Changes in the water surface profile of the Colorado River in Grand Canyon, Arizona, between 1923 and 2000. Water Resources Research 41, W05021. doi:10.1029/2003WR002519.

McKean, J., Roering, J., 2004. Objective landslide detection and surface morphology mapping using high-resolution airborne laser altimetry. Geomorphology 57, 331–351.

Montgomery, D.R., Buffington, J.M., 1997. Channel-reach morphology in mountain drainage basins. Geological Society of America Bulletin 109 (5), 596–611.

O'Callaghan, J.F., Mark, D.M., 1984. The Extraction of Drainage Networks From Digital Elevation Data. Computer Vision, Graphics and Image Processing, 28, 328–344.

Rosgen, D.L., 1994. A classification of natural rivers. Catena 22, 169–199.

Slatton, K.C., Carter, W.E., Shrestha, R.L., Dietrich, W.E., 2007. Airborne laser swath mapping: achieving the resolution and accuracy required for geosurficial research. Geophysical Research Letters 34, L23S10. doi:10.1029/2007GL031939.

Smart, G., Aberle, J., Duncan, M., Walsh, J., 2004. Measurement and analysis of alluvial bed roughness. Journal of Hydraulic Research 42 (3), 227–237.

Staley, D.M., Wasklewicz, T.A., Blaszczynski, J.S., 2006. Surficial patterns of debris flow deposition on alluvial fans in Death Valley, CA using airborne laser swath mapping. Geomorphology 74, 152–163.

Statsoft, 2001. STATISTICA System Reference. Statsoft, Inc., 2300 East 14th Street, Tulsa, Oklahoma, USA. 1098pp.

Storesund, R., Minear, J., 2006. Evaluation of ground-based LiDAR for use in fluvial geomorphology and river restoration. Eos Trans. AGU 87 (52) Fall Meet. Suppl., Abstract G53C-0915.

Tarolli, P., Tarboton, D.G., 2006. A new method for determination of most likely landslide initiation points and the evaluation of digital terrain model scale in terrain stability mapping. Hydrology and Earth System Sciences 10, 663–677.

Wilcox, A.C., Wohl, E.E., 2007. Field measurements of three-dimensional hydraulics in a step-pool channel. Geomorphology 83, 215–231.